

12-2015

Facile sol-gel molten salt synthesis of double perovskite La₂NiMnO₆ as an electrocatalyst for oxygen evolution reactions

Padmini Kukkapalli
The University of Texas Rio Grande Valley

Follow this and additional works at: <https://scholarworks.utrgv.edu/etd>

 Part of the [Chemistry Commons](#)

Recommended Citation

Kukkapalli, Padmini, "Facile sol-gel molten salt synthesis of double perovskite La₂NiMnO₆ as an electrocatalyst for oxygen evolution reactions" (2015). *Theses and Dissertations*. 51.
<https://scholarworks.utrgv.edu/etd/51>

This Thesis is brought to you for free and open access by ScholarWorks @ UTRGV. It has been accepted for inclusion in Theses and Dissertations by an authorized administrator of ScholarWorks @ UTRGV. For more information, please contact justin.white@utrgv.edu, william.flores01@utrgv.edu.

FACILE SOL-GEL MOLTEN SALT SYNTHESIS OF DOUBLE PEROVSKITE $\text{La}_2\text{NiMnO}_6$
AS AN ELECTROCATALYST FOR OXYGEN EVOLUTION REACTIONS

A Thesis

by

PADMINI KUKKAPALLI

Submitted to the Graduate College of
The University of Texas Rio Grande Valley
In partial fulfillment of the requirements for the degree of

MASTER OF SCIENCE

December 2015

Major Subject: Chemistry

FACILE SOL-GEL MOLTEN SALT SYNTHESIS OF DOUBLE PEROVSKITE $\text{La}_2\text{NiMnO}_6$
AS AN ELECTROCATALYST FOR OXYGEN EVOLUTION REACTIONS

A Thesis
by
PADMINI KUKKAPALLI

COMMITTEE MEMBERS

Dr. Yuanbing Mao
Chair of Committee

Dr. Jose J. Gutierrez
Committee Member

Dr. Waseem Haider
Committee Member

Dr. Steven Tidrow
Committee Member

Dr. Tulay Atesin
Committee Member

December 2015

Copyright 2015 Padmini Kukkapalli
All Rights Reserved

ABSTRACT

Kukkapalli, Padmini, Facile Sol-Gel Molten Salt Synthesis of Double Perovskite $\text{La}_2\text{NiMnO}_6$ as an Electrocatalyst for Oxygen Evolution Reactions. Master of Science (MS), December, 2015, 48 pages, 2 tables, 11 figures, 51 references, 45 titles.

Double perovskites e.g $\text{La}_2\text{NiMnO}_6$ have attracted a great attention recently for its high intrinsic activity in oxygen evolution reaction (OER) in electrochemical energy storage and conversion systems in alkaline media. However their stability and specific activity remain challenging that need to be addressed to meet the requirement for OER activities. In this study we synthesized three different samples with varying concentrations via Sol-gel molten salt synthesis by taking molten salts NaNO_3 and KNO_3 in 1:1 molar ratio such as 30:30, 60:60, 90:90 relative to the precursor salts. These samples were characterized by X-ray diffraction, scanning electron microscopes and electrochemical performances. The stability studies were studied by using cyclic voltammogram for multiple cyclings and their Tafel slopes determine the electrochemical reaction to the over potential. The magnetic properties of these compounds allow them as excellent candidates for various applications such as sensors, photovoltaics, memory devices and radio frequency filters.

DEDICATION

The completion of my master studies would not have been possible without the love and support of my family. My mother, Vanajakshi, my father, Srinivasa Rao, my grandmother, Venkatalakshmi, my grandfather, Venkateswarao.

ACKNOWLEDGEMENTS

I express my sincere thanks to my supervisor, Dr. Yuanbing Mao, Associate Professor, Department of Chemistry, UTRGV, for his reverence supervision, eternal support, inspiration and effective criticism throughout my research work. From database funding, research design, and data processing, to manuscript editing, he encouraged me to complete this process through his infinite patience and guidance. My thanks go to my thesis committee members Dr. Jose. J. Gutierrez, Dr. Waseem Haider, Dr. Steven Tidrow, and Dr. Tulay Atesin. Their advice, input, and comments on my thesis helped to ensure the quality of my intellectual work.

I would like to thank Dr. Jason Parson, Department of Chemistry, for guidance in my course work and take care of my scholarships. I would like to thank Dr. Jose J. Gutierrez, Department of Chemistry, for support to my seminar I and seminar II.

I am also thankful to Dr. Madhab Pokhrel, Dr. Bhupendra Bahadur Srivastava for guidance in XRD data analysis and SEM images. I would like to thank Dr. Swati Mohan who guided me to perform the electrochemical analysis. She helped me throughout the analysis and interpretation of electrochemical data. I am also thankful to Lin Wei, Graduate student, of the MAO group research for assistance in Raman data.

I am also sincerely thank to Alfonso Salinas, Department of Mechanical Engineering, for assistance in SEM analysis during my research work.

I would like to thank all the dedicated Multifunctional Application of Oxides (MAO) lab researchers of Department of Chemistry, UTRGV, with special thanks to Dr. Lanhua Yi. I also

want to acknowledge the support of all friends in the Chemistry and Engineering Department, UTRGV.

I would like to gratefully acknowledge the financial support from the Department of Chemistry and funding source for giving me the opportunity to continue the research assistant with Dr. Yuanbing Mao. Also, I would like to acknowledge many volunteers who participated in the focus group research.

I would like to thank Suresh Babu Alaparathi for support in formatting and submitting the final draft of my thesis.

Finally, I would like to thank all the faculty and staff of Department of Chemistry, UTRGV for their help and cooperation.

TABLE OF CONTENTS

	Page
ABSTRACT.....	iii
DEDICATION.....	iv
ACKNOWLEDGEMENTS.....	v
TABLE OF CONTENTS.....	vii
LIST OF TABLES.....	ix
LIST OF FIGURES.....	x
NOMENCLATURE.....	xi
CHAPTER I. INTRODUCTION.....	1
History of transition metal oxides nanoparticles.....	1
Definitions.....	2
Approaches of synthesizing metal oxide nanoparticles.....	2
Rare earth elements.....	3
OER mechanism on perovskite oxide catalysts.....	4
Crystallography.....	6
Characteristics of double perovskites.....	7
Importance of nanoparticles.....	11
Classification of monodisperse magnetic nanoparticles.....	12
Inorganic-inorganic magnetic nanoparticles.....	13
Monodisperse nanoparticle synthesis.....	13
Sol-gel method.....	14
Solvothermal processes.....	14
Co-precipitation.....	15
Motivation of the project.....	15
Research goals of the project.....	16
CHAPTER II. METHODS.....	17

Materials.....	17
Synthesis.....	17
Molten salt synthesis	18
Sol-gel synthesis	18
Sol-gel molten salt synthesis	19
Characteristics	20
X- ray diffraction.....	20
Electron microscopy	20
Raman spectroscopy	21
Electrochemical characterization.....	21
RESULTS AND DISCUSSIONS	22
CHAPTER III. INFLUENCE FACTORS DURING SYNTHESIS.....	36
Anneling Temperature.....	36
CHAPTER IV. CONCLUSION	39
CHAPTER V. FUTURE ENDEAVORS.....	41
REFERENCES	43
BIOGRAPHICAL SKETCH	48

LIST OF TABLES

	Page
Table 1: Tafel slope values of $\text{La}_2\text{NiMnO}_6$ nanoparticle films at different concentrations.....	35
Table 2: Flow chart illustrating factors influencing the molten salt synthesis of a transition metal oxide materials.....	38

LIST OF FIGURES

	Page
Figure 1: Unit cell of a perovskite showing relative positions of different ions.....	4
Figure 2: OER mechanisms proposed for oxide surfaces.....	6
Figure 3: The crystal structure of $\text{La}_2\text{NiMnO}_6$	6
Figure 4: Magnetic dipoles and behavior in the presence and absence of an external magnetic field.....	12
Figure 5: Molten salt synthesis based XRD pattern of $\text{La}_2\text{NiMnO}_6$ nanoparticles.....	23
Figure 6: Sol-gel synthesis based XRD pattern of $\text{La}_2\text{NiMnO}_6$ nanoparticles.....	24
Figure 7: Sol-gel molten salt synthesis based XRD patterns of $\text{La}_2\text{NiMnO}_6$ powders prepared at different concentrations a) 30:30, b) 60:60, c) 90:90	25
Figure 8: SEM images of as prepared a) molten salt , b) sol-gel, c) sol-gel molten salt synthesis a) 30:30, b) 60:60, c) 90:90 concentrations.....	27
Figure 9: Raman spectrum of as-synthesized $\text{La}_2\text{NiMnO}_6$ nanoparticles by a) molten-salt, b) sol-gel, c) sol-gel molten salt synthesis at various concentrations.....	29
Figure 10: OER catalytic performance of sol-gel molten salt synthesis based $\text{La}_2\text{NiMnO}_6$ at various concentrations.....	31
Figure 11: Tafel plot and catalyst mass activities for ohmic and capacitive current corrected OER currents at various concentrations.....	34

NOMENCLATURE

LNMO	:	$\text{La}_2\text{NiMnO}_6$
$\text{Ni}(\text{NO}_3)_3 \cdot 6\text{H}_2\text{O}$:	Nickel (III) nitrate hexahydrate
$\text{Mn}(\text{NO}_3)_3 \cdot 4\text{H}_2\text{O}$:	Manganese (II) nitrate tetrahydrate
$\text{La}(\text{NO}_3)_3 \cdot 6\text{H}_2\text{O}$:	Lanthanum nitrate hexahydrate
KNO_3	:	Potassium nitrate
NaNO_3	:	Sodium nitrate
PVA	:	Polyvinyl alcohol
SEM	:	Scanning electron microscope
TEM	:	Transmission electron microscope
XRD	:	X-ray diffraction
OER	:	Oxygen evolution reactions

CHAPTER I

INTRODUCTION

History of transition metal oxides nanoparticles

The study of these oxides was initiated in the 1950's and since several hundred of these compounds have been produced and studied because they exhibit interesting structural, electronic as well as magnetic properties. Physicist Richard Feynman is considered to be the father of nanotechnology. While at the American Physical Society meeting, held in California Institute of Technology, he presented, "There's plenty of room at the bottom". At this meeting he talked about the ideas and concepts behind nanoscience. He mentioned a process how scientists would be able to manipulate and control individual atoms and molecules. Transition metal oxide (TMO) materials contain transition element and oxygen. Both insulator and metal of poor quality are belongs to this group. It may be happens that the same material may give both types of transport properties. These materials can have unusual and useful electronic and magnetic properties. Many of these properties strongly depend on materials defects like vacancies, dislocations, stacking faults and grain boundaries. Transition metal oxides are used in a wide variety of technologically important catalytic processes. For example, they are used in selective oxidation, selective reduction and dehydrogenation. Understanding surface structure and reactions is important for understanding these catalytic processes. Nanoparticles because of their small size, have distinct properties compared to the bulk form of the same material, thus offering many new

developments in the fields of solar cell, electronics, sensors, photovoltaics, biomedicine and and development of many types of novel products with its potential medical applications on early disease detection, treatment and prevention.

Definitions

Metal oxide: "The metallic compounds which are formed with metal and oxygen in the form of oxide ion (O^{2-}) are called as metal oxide." d-block elements are placed from group-3 to group-12 in periodic table. These all are metallic in nature and also known as transition metals.

Perovskite: A perovskite is any material with the same type of crystal structure as calcium titanium oxide ($CaTiO_3$), known as the perovskite structure with the oxygen in the face centers.

Double perovskite: Double perovskite are the transition metal oxides. They are expressed as $A_2B'B''O_6$, where A is an alkaline (or) rare-earth element and B' and B'' are different transition metal elements.

Approaches of synthesizing metal oxide nanoparticles

There are two general approaches for the synthesis of nanomaterials and fabrication of nanostructures exist: the top-down approach and the bottom-up approach. Top-down approaches use larger (macroscopic) initial structures, which can be externally-controlled in the processing of nanostructures. The top-down approach frequently uses the traditional workshop or micro fabrication methods where tools are used to cut, mill, and shape materials into desired shape and size. Top-down methods include micro patterning techniques such as photolithography and inkjet printing. Bottom-up approaches create composite assemblies from smaller components. These methods use the chemical properties of compounds to cause single molecule components to self-

methods. The desired complexity can be obtained as the assembly is increased. Bottom-up methods are more preferred in the synthesis of nanoparticles.

Rare earth elements

The lanthanide elements are a separate class of fourteen elements in the periodic table including scandium, yttrium and 4f lanthanides. These elements are often known as the rare earth elements. These elements are the group of elements with atomic number increasing from 57(lanthanum) to 71 (lutetium). In the periodic table all rare earth elements are in Group IIIb which are separate group due to the filling of the 4f electron shell. In this series, the atomic radii of the lanthanoid elements become smaller as the atomic number increases. Lanthanum metal is one of the most reactive rare earth elements. It is used to make special optical glasses, including infrared absorbing glass, camera and telescope lenses, other applications for lanthanum include wastewater treatment and petroleum refining. Rare earths are utilized as important elements for high-performance magnets, and are bringing difficulties in dry processes of spent nuclear fuel which are recently drawing attention. However, it is known that current efficiency of the electrolysis of some rare earths such as neodymium is very low for the electrolysis in alkali or alkaline-earth nitrate based metals. For the development of a process to produce pure rare earth metals with high current efficiency, It is important to understand the electrochemical behavior of the rare-earth transition metal oxides. Compared to other type of oxides, a major advantage of double perovskite oxides is the flexibility of their physical-chemical and catalytic properties of the $A_2B_2O_6$ formulation (Fig.1.1) where A sites are rare earth or alkali metal ions and B sites are transition metal ions. Double perovskites have high versatility in their electronic structure and choice of metal cations, advanced perovskites have been progressively developed and modified. The substitution of the A-site and B-site metal cations (Grimaud et al. 2013b; Suntivich et al. 2011a; Chen et al.

2015) [Ni, Mn] and generation of oxygen deficiency/vacancy (Mueller et al. 2015; Hong et al. 2015) have large characteristic effects on their electronic structures and coordination chemistry. As a result, their OER activity is highly correlated to measurable parameters, including number of 3d e_g electrons and their spin state in transition metals, covalency of transition metal-oxygen bond, position of d-band center of transition metal and p-band center of oxygen relative to Fermi level. These measurable parameters depend heavily on the type and distribution of cations and their oxidation states as well as on the concentration of oxygen vacancies.

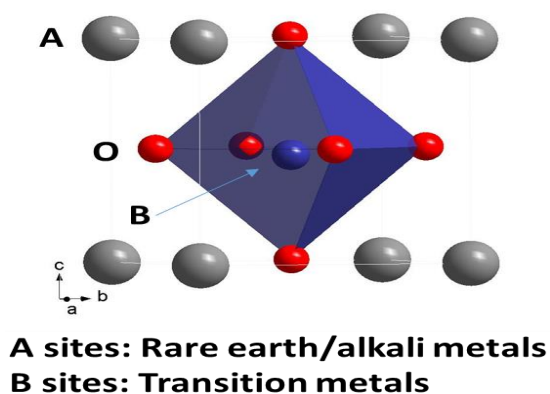
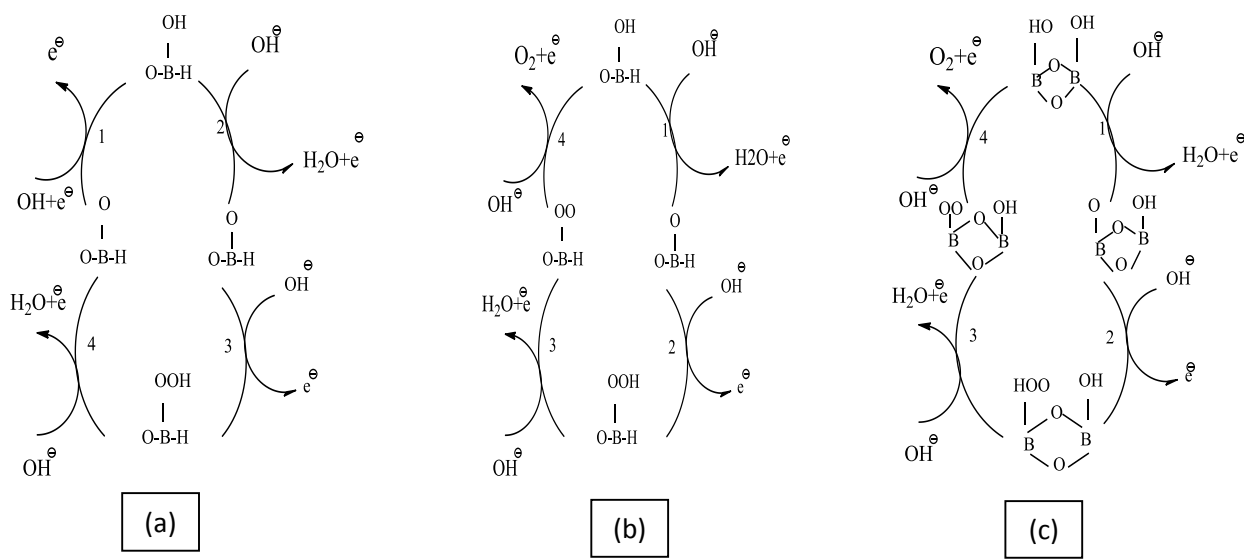


Figure 1: Unit cell of a perovskite showing relative positions of different ions(Chen et al. 2015).

OER mechanism on perovskite oxide catalysts

In 1977, Tseung and Jasem (1977) first studied the criteria for semiconductor oxide electrodes for the OER. They proposed that the oxides having a transition metal redox couple at potentials below the theoretical oxygen electrode can form more active metal sites with higher oxidation state, which would be very promising electrocatalysts. In the following years (1980-1984), Trasatti published a series of interesting workson the OER activity of rutile, spinel and perovskites oxides based upon this criteria.Subsequently, they concluded that these oxides share a common rate-determining step (RDS) *i.e.*, desorption of OH^* intermediates (Trasatti 1980; Trasatti 1984). The anterior activity descriptors laid the foundation for the efficient design of oxide

electrocatalyst over the next 25 years. Figure 2 illustrates some of the proposed reaction mechanisms on oxide surfaces that were resolved from different perspectives. An identical reaction mechanism was proposed as we can observe from (Fig.2a). This mechanism, sometimes alternatively referred to as acid-base mechanism, (Mavros et al. 2014; Betley et al. 2008) essentially proceeds through a series of acid-base steps, in which OH^- , an oxygen nucleophile (Lewis acid), attacks a metal-bound, electrophile oxygen surface species (Lewis base). Computational work on the OER by Mavros and co-workers found that this reaction mechanism is also the most favorable in dimeric metal “oxide” molecules with early transition metal ions (Fig.2c). Whereas, during electrocatalysis of oxygen in alkaline media, these oxides’ surface encounter a pH of 13-14. Suntivich *et al.* proposed that the RDS in reaction mechanisms of OER may be different for different perovskite depending on e_g orbital filling of the transition metal cation (Suntivich et al. 2011b). For example, during OER, for e_g filling greater than 1, RDS is the formation of the O-O bond in OOH adsorbate on B-site cations, whereas for e_g filling less than 1, the deprotonation of the oxyhydroxide group to form peroxide ions may be RDS (Fig.2d) (Suntivich et al. 2011b).



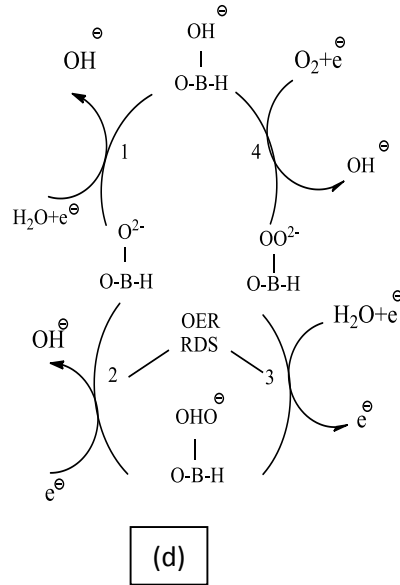


Figure 2: OER mechanism proposed for oxide surfaces. (a) Four-step reaction mechanism proposed by Rossmeisl and co-workers for the OER on noble metal catalyst surfaces(Trasatti 1980)and later applied to oxide surfaces (Suntivich et al. 2011b). (c) Acid-base mechanism proposed for dimeric molecules (Trasatti 1984).(d) Four electron OER reaction mechanism on perovskite surface; the RDS are the O-O bond formation and proton extraction of the oxyhydroxide group.

Crystallography

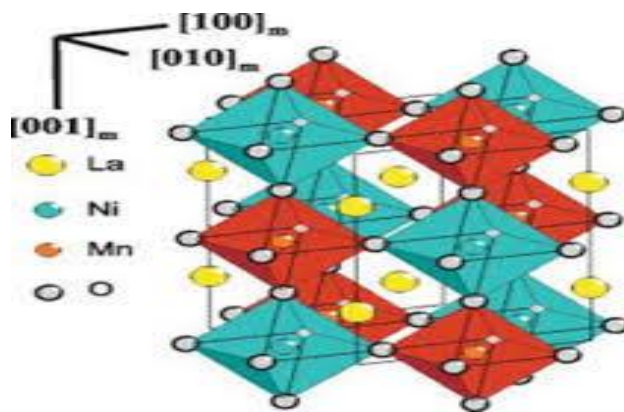


Figure 3: The crystal structure of $\text{La}_2\text{NiMnO}_6$ (Pickett and Moodera 2001).

The double perovskite $\text{La}_2\text{NiMnO}_6$, a magnetic semiconductor, has received considerable attention recently because the material demonstrates ferromagnetic order near room temperature with a Curie temperature (TC) of 280 K (Pickett and Moodera 2001; Wold et al. 1958). With respect to crystal structure, $\text{La}_2\text{NiMnO}_6$ is biphasic with a high temperature rhombohedral phase that transforms at low temperatures to a monoclinic or orthorhombic phase, the final phase depending on the arrangement of the Ni/Mn B-site sub lattice (Pickett and Moodera 2001) BO_6 octahedral forming the backbone of the network and La^{3+} ions filled in the hexagonal holes in the $\text{NiO}_6/\text{MnO}_6$ octahedral. In this Structure La^{3+} ions can be easily replaced by other rare-earth ions. Both La^{3+} and $\text{Ni}^{2+}/\text{Mn}^{4+}$ or $\text{Ni}^{3+}/\text{Mn}^{3+}$ sites can be substituted by a lot of other elements with similar ionic radii in case where electric neutrality is satisfied. The valence band and conduction band of $\text{La}_2\text{NiMnO}_6$ compound consist of La 3d orbital, Mn 2p orbital, Ni 2p orbital and O 1s orbitals. The band structure calculation represents that the La 3d orbitals of $\text{La}_2\text{NiMnO}_6$ lie above the top of the O1s orbitals. The band gap energy of $\text{La}_2\text{NiMnO}_6$ compound size is 300meV lower than $\text{NiO}_6/\text{MnO}_6$ because of the effect of 3d orbitals. A random distribution of Ni and Mn over the octahedral sites of the perovskite structure occurs for rhombohedral (R-3c) and orthorhombic (Pbnm), while an ordering of Ni and Mn into a detectable sites can be accommodated in rhombohedral (R-3 or R-3m) and monoclinic (P21/n) space groups.

Characteristics of double perovskites

Multifunctional materials show various responses to multiple external stimuli enabling novel device applications including intelligent sensors, spintronic, solid state thermoelectric coolers, and other functional devices. For example, double perovskite oxides with general formula $\text{AA}'\text{BB}'\text{O}_6$, where A/A' = rare earth or alkaline earth metals and B/B' = 3d transition metals, display a wide variety of interesting physical properties with composition variations. Considerable research

activity is being carried out to explore new double perovskite materials, to understand the origin of their properties (*e.g.* magnetodielectric, magnetoresistance, magneto capacitance), to improve their properties, and to adapt their materials chemistry to the production technology for each application (Thompson et al. 2015; Ge et al. 2010; Zhang et al. 2014; Zhang et al. 2012). Various perovskites and their related structures have rapidly emerged as promising, highly efficient active materials for applications in solar cell, water splitting device and metal air battery (Bockris and Otagawa 1984; Spendelov and Wieckowski 2007). An important advantage on using perovskites in such these applications, besides the economic benefit by avoiding the use of noble metals, is their flexibility in composition, thus the electronic structures of catalysts. In an ABX_3 (or ABO_3) type perovskite structure, both A and B-sites can vary systematically using metal cations with different valences or ionic radii. Partial replacement or doping at these sites is also relatively straightforward and results in a systematic change of chemical, electronic, and physical properties. For the past several years, a series of perovskites were intensively studied as electro catalysts for oxygen reduction reaction (ORR) and oxygen evolution reaction (OER) in 1970's. since Bockris et al. reported the intrinsic electro catalytic activities of perovskite oxides (Neburchilov et al. 2010; Grimaud et al. 2013a). The eg-filling status of B site metal ions (*e.g.*, Mn, Ni, and) of the perovskites was considered to be critical for high electro catalytic activities in OER based on both the experimental data and theoretical analysis of the electronic structures of molecular orbital's. LNMO, having general structure of double perovskite ($A_2BB'O_6$) is distorted from ideal double perovskite and the amount of distortion changes as the temperature changes (Singh et al. 2007b). The structure of La_2NiMnO_6 is monoclinic with space group $P21/n$. It is a ferromagnetic insulator with Curie temperature, $T_c=280k$. In LNMO, the Ni-d states and Mn-d states suggests the oxidation states to be +2 and +4 respectively. LNMO being an insulator, the ferromagnetism in the

compound is expected to be dominated by the localized super exchange type of interaction of the half-filled d-orbitals of one metal ion with the vacant d-orbital of another metal ion (Singh et al. 2007a). These materials can be prepared by Conventional solid state reactions (Yokoyama et al. 2015), Solid-citrate method (McBain et al. 2008), Hydrothermal method (Tang et al. 2006), Sol-Gel method (Jeong et al. 2007), molten-salt method (Markovich et al. 2011). Recently Alkaline electrolytes have received much attention recently due to facile oxygen evolution and reduction kinetics with earth abundant nonprecious metal oxide catalysts, as alternatives to Pt, IrO₂, and RuO₂ (Lewis and Nocera 2006; Kanan and Nocera 2008). There was a study done on LaNiO₃ which is stable in alkaline electrolytes in the potential region for oxygen evolution and does not exhibit the growth of insulating oxides during electro catalytic activity (Zhou et al. 2006). The previous findings on lanthanum based oxides for OER was done on LaNiO₃ and LaMnO₃ that is ABO₃ type perovskite. The catalytic activity of Lanthanum based perovskites is influenced by various B-site cations and catalytic surface composition has to be investigated by different techniques. General theory behind showing OER activity based on that a near-unity occupancy of the e_g orbital of surface transition metal ions and high covalence in bonding to oxygen can enhance the intrinsic OER activity of perovskite transition metal oxides in alkaline solution.

For the OER, an ideal of e_g just above 1 has been proposed, as observed in materials such as Ba_{0.5}Sr_{0.5}Co_{0.8}Fe_{0.2}O_{3-δ} (BSCF) (Hench and West 1990). In this study, we want to focus on the OER activity of La₂NiMnO₆ because of its potential application towards dielectric properties when compared to rare-earth elements. This oxide has a relatively high theoretical capacity (275 mAh g⁻¹), zero phase change in the voltage range of 2.5-4.4V, Good thermal stability and high safety, less oxygen transparency, better bond coat oxidation resistance, higher thermal expansion coefficient and greater ability to accommodate defects than other rare-earth compounds.

$\text{La}_2\text{NiMnO}_6$ is a ferromagnetic insulator and possesses strong multiferroic properties. This property is occurring due to local Ni/Mn cation ordering. When doping Lanthanum with Ni and Mn its properties has been doubled and show a considerable improvement in its properties such as multicapacitance, multiferroic, magneto dielectric properties (Hench and West 1990; Brinker and Scherer 2013). On this type of material there was lot of research done of studying of its magnetic and dielectric properties. In $\text{La}_2\text{NiMnO}_6$ Ni/Mn displays a paramagnetic-to-ferromagnetic transition at about 300K. It is expected that high-temperature ferromagnetic transition arises from the Ni^{2+} -o- Mn^{4+} super exchange interaction, while the low temperature magnetic transition arises due to the Ni^{3+} -O- Mn^{3+} super-exchange interaction (Demazeau 2008). Further, the ordered phase possesses alternating Ni/Mn and the disordered phase has a random distribution of Ni/Mn cations at B-sites in a typical ABO_3 unit cell.

In the case of double perovskite oxides, the majority of the previous work has focused on $\text{AA}'\text{BB}'\text{O}_6$ single crystals and thin films. However, it can be concluded that the variations mentioned in the study of $\text{La}_2\text{NiMnO}_6$ sample arise from the different synthetic procedures and conditions employed. So far, there are very few reports on $\text{La}_2\text{NiMnO}_6$ and nanostructures. The only most reported synthetic method for $\text{La}_2\text{NiMnO}_6$ nanoparticles is based on a sol-gel process, and few reports on molten-salt synthesis ensuring the formation of Nanostructured $\text{La}_2\text{NiMnO}_6$ spherical particles (Crepaldi et al. 2000; Markovich et al. 2011). These nanoparticles will be analyzed and characterized for the electrochemical properties. These nanostructured components will be prepared by solid-state inorganic materials, subsequently a more stable and strong system in extreme field environments.

This paper considers that the preparation of $\text{La}_2\text{NiMnO}_6$ powder has four advantages: (1) The resulting precipitate derived from nitrous oxides lanthanum nitrate, nickel nitrate, manganese

nitrate is free from contamination, (2) the reaction is carried out under reasonable conditions, (3) the crystalline powders with a small particle-size distribution show lower agglomeration, and (4) the properties of the particles obtained might be different from those particles crystallized at low temperature. In this paper two types of synthesis was carried to obtain $\text{La}_2\text{NiMnO}_6$ nanoparticles, making gel formation by using sol-gel method followed by molten salt synthesis procedure. The molten-salt synthesis is one of the simplest, more versatile, and highly cost-effective approaches available for obtaining crystalline, chemically pure, single-phase nanoscale materials at lower temperatures and often in overall shorter reaction times with little residual impurities as compared with conventional other synthesis methods. The Sol-gel molten salt synthesis of $\text{La}_2\text{NiMnO}_6$ was a new approach to obtain pure phase nanoparticles which we can avoid agglomeration and obtaining uniform sized crystalline particles.

Importance of nanoparticles

Nanoparticles constitute of layers and shells of variant compositions depending on the application for which the particle is being synthesized. Nanometersizeeffect plays a crucial role for determining the properties of the materials. Nanoscaling laws of magnetic nanoparticles are important not only for understanding the behavior of existing materials but also for developing novel nanomaterials with superior properties. Nanoparticle characterization is necessary to establish understanding and control of nanoparticle synthesis and theutilization in a variety of applications ranging from storage media for magnetic memory devices to probes and vectors in the biomedical sciences (Demazeau 2008), quantitative immunoassay, and hyperthermia (Crepaldi et al. 2000). The monodisperse and magnetic composite materials have attracted good optical performance for application.

ferromagnetic materials, the atomic level magnetic dipole moments are similar to those of ferromagnetic materials, however, adjacent dipole moments exist that are not oriented in parallel and effectively cancel or reduce, respectively, the impact of neighboring magnetic dipoles within the material in the absence of an applied field. In the case where the magnetization of the MNP over the measurement/observation interval is equal to zero in the absence of an external field, such nanoparticles are referred to as super paramagnetic.

Inorganic-inorganic magnetic nanoparticles

Among the types of monodisperse magnetic nano-particles, inorganic-inorganic nanoparticles are the most important class. These types of particles are widely used for the improvement of semiconductor efficiency, magnetic storage media, information storage, photovoltaics, and sensors. Use of metal oxide nanoparticles to improve performance of oxide thin films as conducting media in commercial gas and vapor sensors. The inorganic-inorganic monodisperse components are made up of metal, metal oxides, semiconductors and any other inorganic compounds. Metal oxides with $\text{La}_2\text{NiMnO}_6$ tend to be monodisperse particles with good optical performance. These particles have enhanced dielectric properties. Monodisperse nanoparticles are used to improve the efficiency of many electrochemical technologies in reaching of sustainable energy, such as water splitting (Kim et al. 2014) and rechargeable metal-air batteries (Iliev et al. 2003).

Monodisperse nanoparticle synthesis

Monodisperse Magnetic nanoparticles are made from metal-salt co-precipitation method. To produce these nanoparticles, a burst nucleation should occur in a supersaturated solution without the formation of new nuclei and growth of these particles should be uniform. Control of the size and nucleation growth factor are the key points to consider in obtaining of these

nanoparticles. Uniformity of the particle size distribution is only achieved through a short nucleation period that produces all the particles obtained at the end of reaction. For inorganic particle synthesis, the molten salt, hydrothermal, sol-gel and chemical precipitation reactions in bulk aqueous system are common techniques. For obtaining metal-oxide particle synthesis the use of sol-gel method is preferred (Stoerzinger et al. 2015).

Sol-gel method

The sol-gel synthesis is a chemical solution process widely used in the fields of material science and ceramic engineering for mainly metal oxide particle synthesis. It uses either a chemical solution or colloidal particles to produce an integrated network (gel). The sol-gel process is an effective method for preparing such materials since the reactants can be homogeneously mixed at the molecular level in solution. Sol-gel processing is synthesis of colloidal dispersions of inorganic and organic-inorganic hybrid materials. From these colloidal dispersions, powders, fibers and thin films can be prepared. The sol-gel technique allows for a low processing temperature and yields molecular level homogeneously (Martín-Carrón et al. 2002).

Solvothermal processes

The solvothermal method can be described as a chemical reaction or a transformation of precursors in the presence of a solvent in a closed system and at a temperature higher than the boiling temperature of the solvent. Consequently, pressure is involved. Two different cases are possible: (i) pressure is autogeneous and closely dependant of the percentage of filling for the reaction vessel and of temperature, (ii) Pressure is imposed. Solvothermal processes are governed by different key factors: i) the composition of the reactants, (ii) the nature of the solvent (in particular its physico-chemical properties), (iii) the additives used and (iv) the thermodynamic parameters: temperature and pressure (Guo et al. 2006).

Co-precipitation

Co-precipitation reactions involve the simultaneous occurrence of nucleation, growth, and agglomeration process. Here nucleation is a key step, and a large number of small particles will be formed. In this technique, pH-control conditions can be used during the precipitation step. The pH-values are kept constant throughout co-precipitation because magnetic properties of the material depend on the crystal size and the degree of agglomeration of individual nanoparticles. Such agglomeration appears to be responsible for the formation of mesoporous structures, which are affected by the pH, the nature of alkali, the slow or fast addition of alkaline solution. High crystallinity, high surface area and average pore diameter of the particle size will be obtained by maintaining the constant pH conditions. When variable pH are compared, the co-precipitation method with constant pH has been used to obtain high crystallinity, phase purity and homogeneity of the material (Nishio et al. 2007).

Motivation of the project

In the past decade, most researchers focused on different methods for monodispersed nanoparticle synthesis. For example molten salt synthesis is a widely studied method due to its advantages in controlling of particle size and shape. In molten salt synthesis, the mixing of salt and precursors is an important factor to maintain proper composition for formation of desired nanostructured compounds. Salt medium will also play an important role in the formation of nanoparticles. In this project, challenge has been overcome to synthesize lanthanum manganese nickel nitrate oxide nanoparticles. The size of the nanoparticles was controlled in presence of salt medium.

Research goals of the project

The main goals of this study are to prepare the uniform size monodispersed magnetic nanoparticles and to increase its functionality, stability and dispersal abilities. This kind of nanoparticles have broad applications as sensors, photovoltaic's, dielectrics, energy storage batteries and electricity-driven solar water splitting, electrocatalysts for oxygen evolution reaction:

My research work deals with the use of sol-gel and molten salt synthesis to create the nanostructured $\text{La}_2\text{NiMnO}_6$ monodisperse nanoparticles. It is expected to demonstrate strong electrocatalytic properties from the spherical nanostructured samples.

The specific goals are

1. To optimize the change in lanthanum manganese nickel oxide nanoparticles size with variation of salt medium in the presence of precursors.
2. To achieve uniform size of monodispersed nanoparticles of lanthanum manganese nickel oxide and to calculate the overall nanoparticle size by Scherer analysis.
3. To examine the electro catalytic performance of lanthanum manganese nickel oxide nanoparticles in oxygen evolution reactions.
4. To determine its stability and activity to withstand its electro catalytic behavior.
5. Characterization of the lanthanum manganese nickel oxide nanoparticles by XRD, SEM, RAMAN and Electrochemical performance data.

CHAPTER II

METHODS

Materials

The starting materials were $\text{La}(\text{NO}_3)_3 \cdot 6\text{H}_2\text{O}$ (99.99%), $\text{Mn}(\text{NO}_3)_3 \cdot 5\text{H}_2\text{O}$ (99.99%), $\text{Ni}(\text{NO}_3)_2 \cdot 6\text{H}_2\text{O}$, NaNO_3 (98%), KNO_3 (99%), Polyvinyl alcohol PVA (99%), KOH, Polyvinylidene fluoride (PVDF) from Alfa Aesar, USA. Dimethylformamide (DMF), Carbon black, was obtained from Sigma Aldrich, USA.

Synthesis

Synthesis of $\text{La}_2\text{NiMnO}_6$ was carried out by three procedures.

- 1) Molten salt synthesis
- 2) Sol-gel synthesis
- 3) Sol-gel molten salt synthesis

In a typical synthetic protocol a single-complex precursor was prepared by using above three procedures. In this study we developed a new synthetic case study of obtaining $\text{La}_2\text{NiMnO}_6$ nanoparticles by using sol-gel molten salt synthesis which it was not studied elsewhere. The details of this procedure will be studied later.

The detailed study of synthesis procedures.

Molten salt synthesis

In a typical sample preparation protocol of La_2BMnO_6 (B = Ni or Co in this study) nanocrystals, high-purity lanthanum nitrate, nickel or cobalt nitrate, manganese nitrate, sodium nitrate, and potassium nitrate were mixed in a molar ratio of 2 : 1 : 1 : 60 : 60 and ground for 30 min with aid of ethanol. The mixture was then placed within a covered nickel crucible, which was subsequently placed inside a box furnace and heated to 700 °C at a ramp rate of 2°C/min⁻¹. After isothermal annealing at 700°C for 6 h, the resulting mixture was cooled to room temperature at a ramp rate of 5°C/min⁻¹. The resulting sample was subsequently purified with extensive amounts of distilled water followed by centrifugation. The remaining precipitate was heated at 80°C overnight in a drying oven. The collected samples was taken and then grinded to form fine powder and characterized by using XRD analysis (Mao 2012).

Sol-gel synthesis

The precursor solution was prepared by using $\text{La}(\text{NO}_3)_3 \cdot 6\text{H}_2\text{O}$, $\text{Ni}(\text{NO}_3)_2 \cdot 6\text{H}_2\text{O}$, and $\text{Mn}(\text{NO}_3)_2 \cdot 4\text{H}_2\text{O}$. Stoichiometric amount of the salts were dissolved in 8ml distilled water. The mixture was continuously stirred for 2hr. A polyvinyl alcohol (PVA) was prepared by taking 0.25gm PVA in a beaker containing 20ml distilled water. The mixture was stirred continuously and the temperature raised gradually to 350k. The stirring was contained until PVA was completely dissolved in water. The two solutions prepared as above (viz., $\text{La}(\text{NO}_3)_3 \cdot 6\text{H}_2\text{O} + \text{Ni}(\text{NO}_3)_2 \cdot 6\text{H}_2\text{O} + \text{Mn}(\text{NO}_3)_2 \cdot 4\text{H}_2\text{O}$ and PVA, respectively) were mixed with a volume ratio 5:2. The final solution was allowed to form a clear solution at room temperature. The resulting gel was dried in oven. The product was then heated to 693K, and thereafter furnace cooled to room temperature. These heating and cooling cycles were repeated three times to remove organic PVA. The resultant powder was

subjected to heat treatment at 1148K for 1h to grow the required crystalline phase (Maiti et al. 2012).

Sol-gel molten salt synthesis

This was the modified method of above two methods which was a new synthesis approach in the preparation of double perovskites. The precursor solution was prepared by using $\text{La}(\text{NO}_3)_3 \cdot 6\text{H}_2\text{O}$, $\text{Ni}(\text{NO}_3)_2 \cdot 6\text{H}_2\text{O}$, and $\text{Mn}(\text{NO}_3)_2 \cdot 4\text{H}_2\text{O}$. Stoichiometric amount of the salts were dissolved in 8ml distilled water. The mixture was continuously stirred for 2hr. A polyvinyl alcohol (PVA) was prepared by taking 0.25gm PVA in a beaker containing 20ml distilled water. The mixture was stirred continuously and the temperature raised gradually to 350k. The stirring was continued until PVA was completely dissolved in water. The two solutions prepared as above (viz., $\text{La}(\text{NO}_3)_3 \cdot 6\text{H}_2\text{O} + \text{Ni}(\text{NO}_3)_2 \cdot 6\text{H}_2\text{O} + \text{Mn}(\text{NO}_3)_2 \cdot 4\text{H}_2\text{O}$ and PVA, respectively) were mixed with a volume ratio 5:2. The final solution was allowed to form a clear solution at room temperature. The resulting gel was dried in an oven. Then after 0.35gm of the resultant gel was taken and mixed with different nitrate salts such as potassium nitrate and sodium nitrate (1:1) ratio. Here we synthesized three different types of concentrations such as taking different concentration of $\text{KNO}_3:\text{NaNO}_3$ (30:30, 60:60, 90:90) and then followed by molten salt synthesis method. The mixture was then placed within a covered nickel crucible, which was subsequently placed inside a box furnace and heated to 700 °C at a ramp rate of $2^\circ\text{C}/\text{min}^{-1}$. After isothermal annealing at 700°C for 6 h, the resulting mixture was cooled to room temperature at a ramp rate of $5^\circ\text{C}/\text{min}^{-1}$. The resulting sample was subsequently purified with copious amounts of distilled water followed by centrifugation. The remaining precipitate was heated at 80°C overnight in a drying oven. The collected samples were taken and then grinded to form fine powder and characterized by using XRD analysis (Mao 2012; Maiti et al. 2012).

Characteristics

X- ray diffraction

The crystalline structure of the powders was determined using X-ray diffraction with Cu K α radiation at room temperature by plotting the angular and intensity measurements. The XRD data for the powder samples were examined on a Rigaku-MiniflexTM II X-ray diffractometer using Cu K α radiation ($\lambda = 0.1549\text{nm}$). The generator voltage and current was set at 35KV and 25mA respectively. The samples were scanned in the 2θ ranges 10° to 90° range in continuous scan mode. The scan rate was $1^\circ/\text{min}$ and step width 0.01° (2θ). Phases present in the samples has been identified with the search match facility available with standard measurements software.

Phases present in the sample has been identified with the search match facility available. The crystallite size of the calcined powders was determined from X-ray line broadening using the Scherrer's equation as follows.

$$D_{\text{HKL}} = K\lambda / \beta \text{Cos } \theta$$

Where, D_{HKL} = the size along the (hkl) direction

$$K = \text{Constant}(0.90)$$

$$\lambda = \text{Wavelength of the Radiation}$$

$$\theta = \text{Bragg's angle and}$$

$$\beta = \text{full width at half maximum}$$

Electron microscopy

The particle size and morphology of the resulting products were initially characterized using a SEM (ZEISS EVO LS10), smart SEM software at accelerating voltages of 2kV. The SEM is used to identify the shape and surface of the sample by using ZEISS EVO LS10, smart SEM software. Specifically, samples were deposited onto conductive copper tape on to carbon

conductive tape, which were then attached to the surfaces of SEM brass stubs, so to as minimize charging effects under SEM imaging conditions. For the creation of nameplates samples were initially attached to a piece of double-sided conductive carbon tape copper tape was then used. Specimens for low magnification.

Raman spectroscopy

Raman spectra of powder were recorded from 50 to 900 cm^{-1} with a 4 cm^{-1} spectral resolution on a microscope SENTERRA with laser protective enclosure by signal of CCD detector. The OPUS software is used for instrument control, data acquisitions, manipulation and evaluation.

Electrochemical characterization

The oxygen evolution reaction activities of $\text{La}_2\text{NiMnO}_6$ were evaluated by Rotating disk electrode (RRDE) setup using a glass electrochemical cell with silver chloride electrode as a reference electrode (Ag/AgCl) and platinum counter electrode (all from Pine Instruments). The potentiostat / galvanostat PSTAT302N portable mini is small, compact and easy to use and allows to use all the basic electrochemical techniques such as the changes of surface or to study reactions and kinetics electron transfer. By using NOVA software we can analyze the experimental data and simulation of cyclic voltammogram data. A three-electrode cell configuration was used. The working electrode was a glassy carbon rotating disk electrode (RDE) with an area of 0.07cm^2 . The working electrodes were composed as below: the calcined $\text{La}_2\text{NiMnO}_6$ nanoparticles were first evenly grinded with carbon black and polyvinylidene fluoride (PVDF) with a weight ratio of 80:10:10 in dimethyl formamide (DMF). And then the prepared working electrodes were placed on glassy carbon electrode (Nishio et al. 2007). Freshly prepared metal oxide catalysts ink was deposited on glassy carbon rotating disk electrodes (RDEs). The electrolyte resistance was

measured under the oxygen gas was found to be for the same electrolyte solution to ensure the accuracy. All the data were collected within 4hr to minimize any side reactions. Cyclic voltammograms (CVs) were obtained at 1600rpm under ambient room temperature to obtain OER currents. The scan rate was set at 10mv/s and the scan range was from 1.1 to 1.8 V. Three independent measurements were carried out for each catalyst. The analysis of OER kinetic currents was capacitance-corrected by taking the average between positive and negative-going scans and then iR-corrected. Potentials in this study are referred to the RHE potential scale and correspond to applied potentials, unless they are stated to be iR-corrected, denoted as E-iR, where i is the current and R is the electrolyte resistance and it was found to be 50Ω (Kim et al. 2014).

RESULTS AND DISCUSSIONS

Previous research on La₂NiMnO₆ synthesis involved sol-gel, molten-salt, hydrothermal, co-precipitation and pulser laser deposition methods. But mostly used synthesis was based on the sol-gel based method which we can able to get the uniform size of the particles. All these synthesis process produced large particles greater than 30nm and smaller surface-area to volume ratio.

In our study, three types of synthesis was performed sol-gel, molten salt and sol-gel molten-salt synthesis and out of these methods the third method achieved less particle size which is pure with no detectable impurities. These diffraction lines observed at 2θ angle 22.24°, 32.45°, 41.82°, 46.67° 53.5°, 58.89°,67.32°, have been indexed as (002), (200,020), (121,202,113), (220), (114,130), (024,132), (224,040) respectively, these peaks as characteristic of Lanthanum nickel manganese oxide structure. The XRD patterns were analyzed to determine peak intensity, position and width. Full-width at half-maximum (FWHM) data was used, and the average particle size was estimated using Scherer equation (discussed in 'Material and Methods' Section). The typical XRD pattern revealed that the sample contains a single polycrystalline orthorhombic phase structure of

Lanthanum nickel manganese oxide nanoparticles. The average estimated particle size of this sample was 20nm for molten salt synthesis, 26nm for sol-gel synthesis prepared sample and 14-15nm for sol-gel molten salt synthesis prepared samples.No obvious XRD peaks arising from impurities were found, meaning that $\text{La}_2\text{NiMnO}_6$ nanosphereswas successfully synthesized with high purity. By indexing the XRD patterns, the data from our as synthesized $\text{La}_2\text{NiMnO}_6$ were shown in Figure 5.

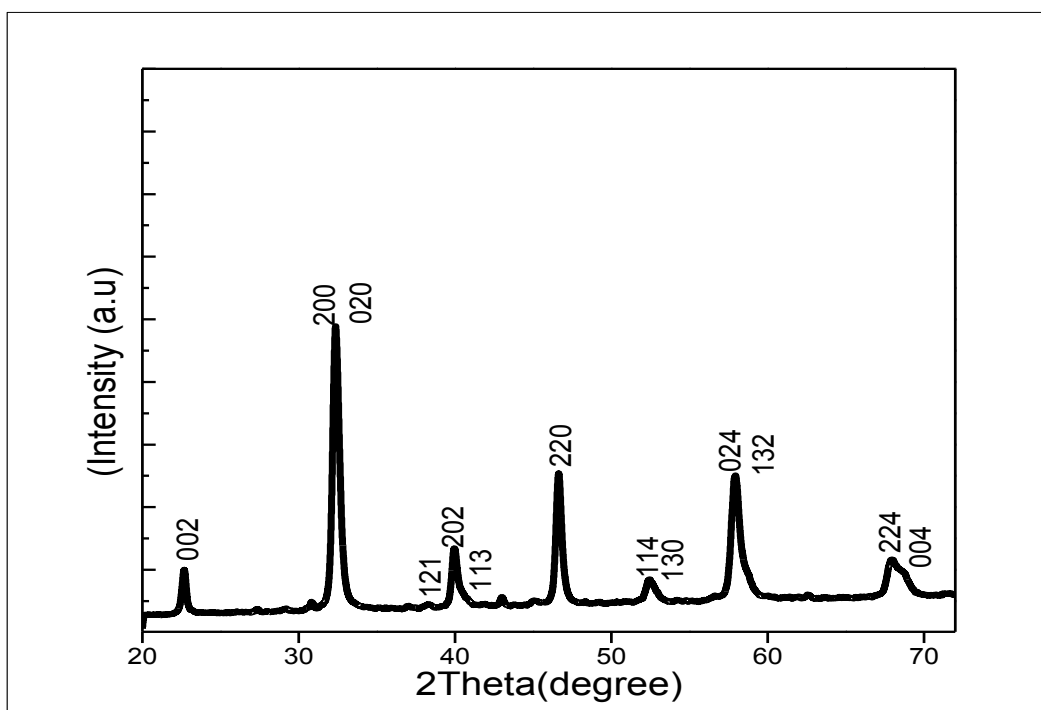


Figure 5: Molten salt synthesis based XRD pattern of $\text{La}_2\text{NiMnO}_6$ nanoparticles

As shown in Figure 6 as prepared $\text{La}_2\text{NiMnO}_6$ particles, no extra reflection peaks other than those of pure perovskite phase are observed within the experimental limit, which confirms the formation of single phase composition double perovskites. Based on the Scherer analysis calculated the crystallite domain size was found to be 20nm which was carried at higher temperature i.e at 650K.

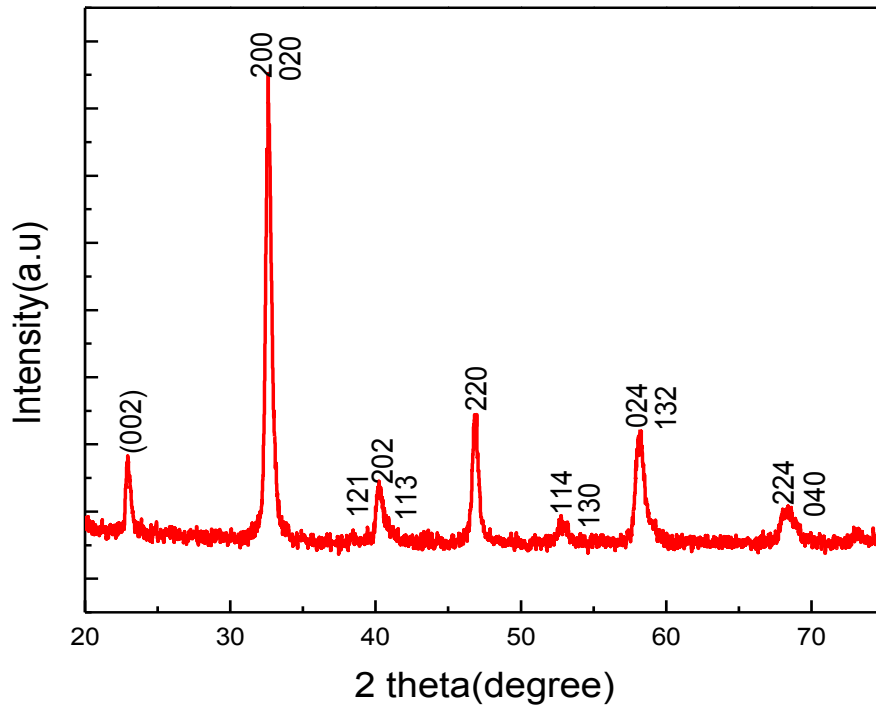


Figure 6: Sol-gel synthesis based XRD pattern of $\text{La}_2\text{NiMnO}_6$ nanoparticles

As shown in Figure 7 as prepared $\text{La}_2\text{NiMnO}_6$ particles, no extra reflection peaks other than those of pure perovskite phase are observed within the experimental limit, which confirms the formation of single phase composition double perovskites. Based on the Scherrer equation, the calculated crystalline domain sizes are 14nm for (30:30), 14.2nm for (60:60), 15nm for (90:90) concentrations which is less than the particle size less than the sol-gel, molten salt synthesis methods.

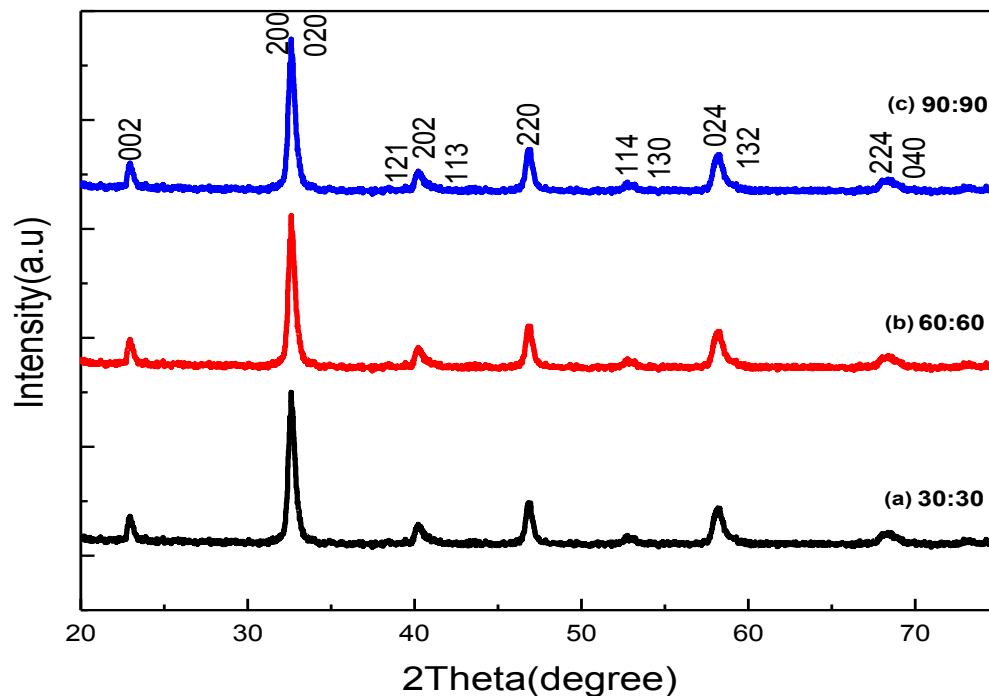


Figure 7: Sol-gel molten salt synthesis based XRD patterns of $\text{La}_2\text{NiMnO}_6$ powders prepared at different Concentrations a) 30:30, b) 60:60, c) 90:90.

The sizes and morphologies of as prepared samples were examined by scanning electron microscope technique. Figure 8 shows the SEM images of as prepared nanoparticles by different routes such as molten salt, sol-gel, and sol-gel molten salt synthesis. Figure 8(a) shows the molten salt synthesis nanostructures, prepared at temperature of 700°C are spherical and quite uniform. Figure 8(b) shows the sol-gel synthesis nanostructures, prepared at 650K shows crystalline samples and uniformed samples. Figure 8(c,d,e) shows the sol-gel molten salt synthesis samples, prepared at 700°C which are spherical and unioordered samples. The average particle size of these samples are found to be Figure 8a) 26nm , b) 20nm , C) 14nm , d) 14.2nm , e) 15nm . The results above suggesting that the combination of sol-gel molten salt synthesis samples produce less than 20nm particle size which associate together, showing the advantage of this new approach of the as

prepared nanoparticles in the synthesis of oxide catalysts. The gel can reduce the diffusion ion path lengths without generating mixed phases and molten salt mixture used act as a separator between the formed nanoparticles or surfactant of the nanoparticles surface. Poly vinyl alcohol is a synthetic polymer acts as adhesive and increases the crystallinity and high oxygen diffusion forming films. The reaction time 700° C did not seem to be too high for maintaining the morphology. The advantage of this method is we can produce nanoparticles which are non-aggregated with narrow size distribution during the nanoparticle growth process and even during the cooling process. In order to have the good catalytic activity lesser nanoparticle size particles are preferred because they can produce the more surface area with small size and maintain good stability compared to larger particles with smaller surface area.

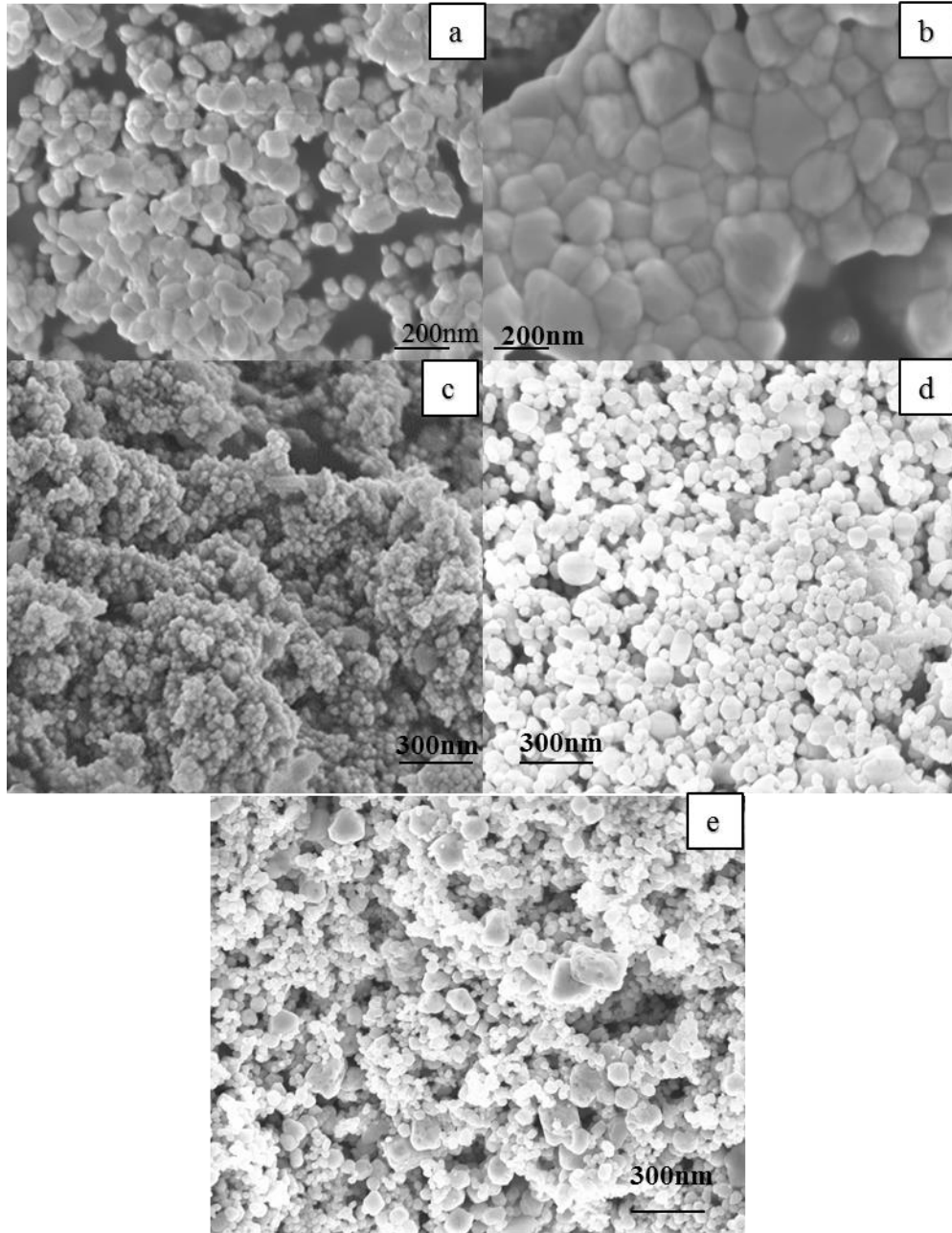


Figure 8: SEM images of as prepared a) molten salt, b) sol-gel, c) sol-gel molten salt synthesis of 30:30, d) 60:60, e)90:90 concentrations of $\text{La}_2\text{NiMnO}_6$ nanoparticles.

In Figure 9 shows the Raman spectra from different $\text{La}_2\text{NiMnO}_6$ nanoparticle synthesis obtained by molten-Salt, sol-gel and sol-gel molten-salt synthesis. In Figure 9a,b,c the Raman spectra are dominated by two broad peaks at around 524 and 670cm^{-1} , which can be assigned to

the A_g antisymmetric stretching (or Jahn-Teller Stretching mode) and B_g symmetric stretching vibrations of the MnO_6 octahedra, respectively. A noticeable difference is seen between our La_2NiMnO_6 nanoparticles and the bulk sample: The A_g and B_g peaks for the nanoparticles shift to the higher energy, 3 and 9cm^{-1} , respectively, when compared to the bulk crystal. These type of phase changes occur with decreasing film depositing oxygen pressure (Rogado et al. 2005). These phenomena are attributed to the fact that the symmetric stretching mode in the $P2_1/n$ is fully symmetric and involves both the in-plane and out-of-plane stretching vibration of the MnO_6 and NiO_6 , while the antisymmetric stretching mode primarily involves only in-plane antisymmetric vibrations. As a result, the symmetric stretching mode and anti-stretching mode shift in the opposite directions. The increase in the out-of-plane lattice parameter with decreasing particle size. The peak shifts occur due to surface strain from the nano-sized particles.

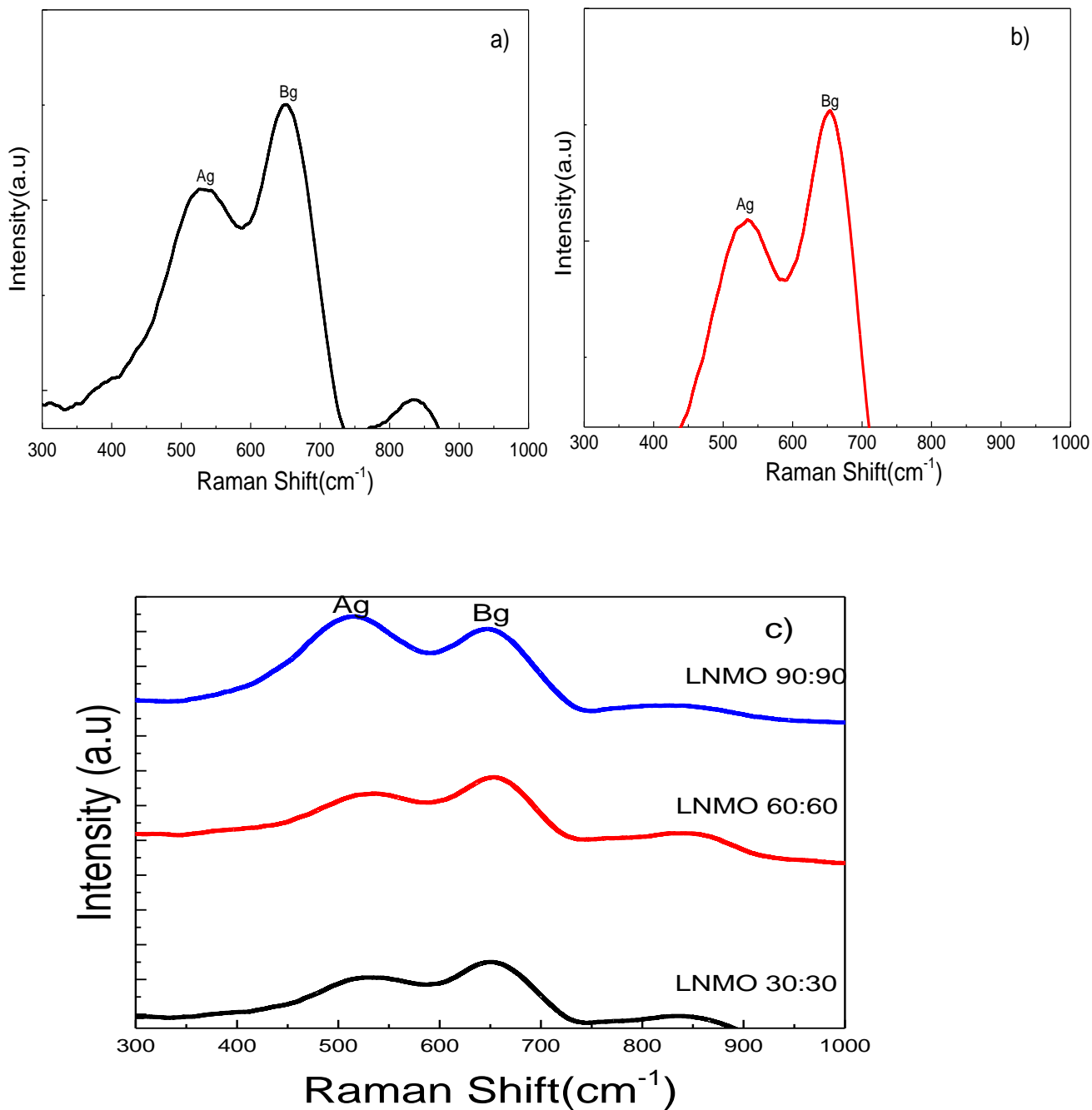


Figure 9: Raman Spectrum of as synthesized $\text{La}_2\text{NiMnO}_6$ nanoparticles by a) Molten-salt synthesis b) Sol-gel synthesis c) Sol-gel molten salt synthesis at 30:30, 60:60, 90:90 concentrations.

A rotating ring disk electrode (RRDE) study was carried out to examine the origin of the observed currents. To assess their OER catalytic activity, our materials was first loaded onto glassy

carbon electrode, in 0.1M KOH aqueous electrolyte. Fig 10 illustrate the ohmic drop (iR) corrected anodic cyclic voltammogram (CV) scans of $\text{La}_2\text{NiMnO}_6$ nanoparticles prepared at three different concentrations in O_2 -saturated 0.1M KOH at a scan rate of $10 \text{ mV}\cdot\text{s}^{-1}$ in the range of 1.0-1.8V Ag/AgCl electrode. A total of 25 cycles for each electrode composition was performed to evaluate the effect of potential cycling on the OER activity. The cyclic voltammetry (CV) curve of LNMO 30:30 exhibit more positive OER peak potential and higher peak current than 90:90 and 60:60. The LNMO 30:30 and 60:60 showed a significant decrease in the OER current upon cycling, while 90:90 showed a increase in the peak current which was due to minor changes occurred in the capacitive currents. The increase or decrease of the peak current was determined by using the Tafel plot (Rogado et al. 2005). From the Tafel slope we can determine the how much applied voltage influenced the forward reaction alpha used for multistep electron process. The fundamental reason for the differing behaviour arising from the oxide growth methods is still unknown. The clear fact to be known is that extent and rate of growth varies depend on the synthesis method used such as effect of concentration, particle size, and temperature. From Fig 2.6 30:30 showed increased current which was due to lesser particle size than 60:60 and 90:90. But for 90:90 this is quite uncommon as it showed increased current density but under repetitive cycling it cannot withstand its stability, this is due to increasing in the number of particle size leads to decreasing the surface area and having lesser collision between the particles which will decrease the activation energy and which effects the reaction kinetics. Due to these reasons, the material have less chances of maintaining its stability. For 60:60 as it is showing lesser peak current but under multiple cycling this material maintained a constant stability which is good for OER.

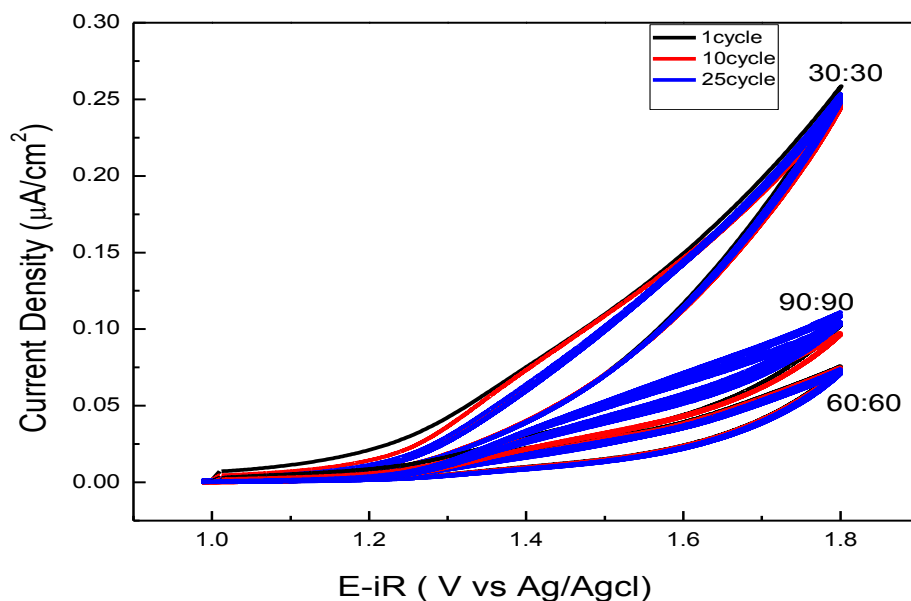


Figure 10: Oxygen evolution catalytic performance of Sol-gel molten-salt synthesis based $\text{La}_2\text{NiMnO}_6$ nanoparticles at 30:30, 60:60, 90:90 concentrations on glassy carbon electrodes in O_2 saturated in aqueous electrolyte, 0.1M KOH with a speed of 1600-rpm and sweep rate of 10mv/s.

Figure 11 represents the tafel plots and catalyst mass activities for three different samples such as LNMO 30:30,60:60, 90:90 and the Tafel slope values were listed in table1 at 1 and 25cycles. For all the three samples as we consider the multiple cycling the tafel slopes does not vary significantly. In figure 11d) the mass activity defined as the current density achieved per metal mass loading at 1.57 V vs Ag/AgCl for all the three tested electrodes in the first and the 25th cycle are outlined. LNMO 30:30 sample showed the highest activity among 60:60 and 90:90. This was due to having higher surface area compared to 60:60 and 90:90. In addition, changes in the capacitive region are even smaller for all the three samples. It is notable fact that nickel-perovskite cathode materials are generally more stable at high temperatures and it can withstand its stability (Rincón et al. 2014). There were less reports on lanthanum based perovskites in case of

studying the OER catalytic activities. We are the first to report the OER activities of $\text{La}_2\text{NiMnO}_6$. Stability and intrinsic mass activity are the concerns that we need to take into consideration in the development of new catalyst for improving the OER performance. But in case of $\text{La}_2\text{NiMnO}_6$ under repetitive cycling for 25 cycle there was decrease in the current density as we seen. But this change was minimal and acceptable. As if we compare the mass activity individually for samples LNMO30:30 stood $\sim 0.13 \mu\text{A}/\text{cm}^2_{\text{oxide}}$ and 60:60 fall to $\sim 0.03 \mu\text{A}/\text{cm}^2_{\text{oxide}}$ which is nearly 10 times less than 30:30 and 90:90. From this we can able to conclude that among all there is minimal changes in comparision and 90:90 shows a increase in the mass activity upon increasing in the cycling which may be due to surface change in the morphology due to amorphization. There was recent study on LSCF perovskites which showed increase in its stability at lower temperatures in alkaline environment. By taking this fact into consideration it might be assumed that the presence of La lattice structure, coupled with the reduction in Ni and Mn content stabilizes the lattice of the oxide during OER experiments to a greater extent than for the oxides with the Co content such as BSCF (Jin et al. 2010). There was recent finding on the universal dependance of the OER activity on the oxygen binding strength, the work on double perovskites proposed that the e_g filling of surface transition metal cations can greatly influence the binding of OER intermediates to the oxide surface and thus the OER activity. In that study they proposed that BSCF material shows increased in its current density under multiple cyclings but this material loss the stability for a long time because under repetitive cyclings the material undergoes changes in its surface amorphization which is good for OER for a short period of time, they also mentioned that LaMnO_3 material shows less reduction in its surface morphization but shows a improved performance for a prolonged time. By examingthis evidence as we see from Tafel slopes intially it showed increasing in its current which was in microamperes and still remained constant under multiple cyclings which we

might assume that this material is good in maintaining its stability and activity. The improvement of OER catalysts may strongly depend on the e_g filling of surface B-cations, where the activities are compared in terms of the overpotential required to produce a specific current. However, in accordance with the above results demonstrate that the active chemistry and structure of oxide catalysts during OER can significantly differ from those of as-synthesized material and understanding how the oxide surface may change and impact the OER activity is critical to the design of highly active and stable OER catalysts. So choosing A-site and B-site transition metal atoms also play a crucial role in the design of good OER electrocatalysts.

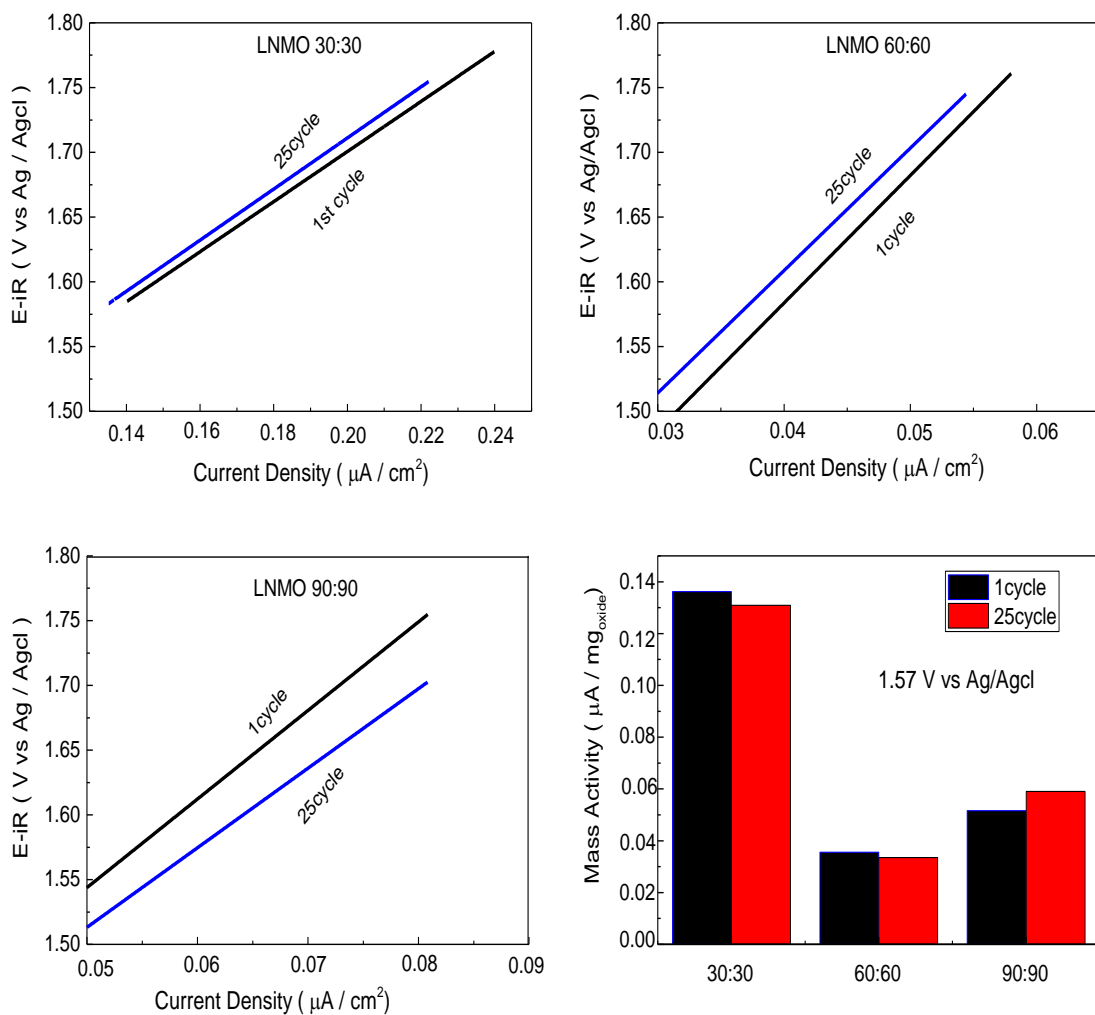


Figure 11: Tafel plot for ohmic and capacitive current corrected OER currents obtained from a scan at 10 mV/s and 1600 rpm for a) 30:30, b) 60:60, c) 90: 90 at 1,10,25 cycles d) catalyst mass activities for the oxide metals loading in the electrode at a potential of 1.57 V vs Ag/AgCl for the (1&25cycles) for each electrode material.

Table 1. The Tafel slope values obtained in mv/dec for a series of $\text{La}_2\text{NiMnO}_6$ films at different concentrations i.e, LNMO at 30:30, 60:60, 90:90 prepared using 25 growth cycles via Sol-gel molten salt synthesis method.

Number of cycles	LNMO30:30	LNMO 60:60	LNMO 90:90
1	104	198	176
10	103	197	178
25	103	196	169

Nanostructured transition metal oxides exhibit excellent properties, such as ferromagnetic, ferroelectric and photovoltaic properties. Double perovskites are belong to the transition metal oxides class of materials which provide one of the greatest potentials for improving performance and used in a wide range of potential applications including microelectronics, energy storage, sensors and biomedicine due to their tunable chemical and physical properties. Compared to nanostructures there are other class of materials associate are nanocrystalline materials and nanocomposites. Nanoparticles and nanostructures have been shown better performance in absorption of light, increase the conversion of light to electricity, and provide better thermal storage and transport. Nanostructured materials explosion in both academic and industrial interest in these materials over the past decade arised from the remarkable variations in industrial interest in fundamental electrical, optical and magnetic properties (Tsipis and Kharton 2011). Therefore, Lanthanum based double perovskites have excellent properties for maintaining its stability, activity and superconductive behavior of oxides.

CHAPTER III

INFLUENCE FACTORS DURING SYNTHESIS

Anneling Temperature

Annealing temperature plays a crucial role for synthesizing nanomaterials. The solubility and reactivity of precursors increase with the increasing temperature i.e. annealing reaction time, the solvent we used. Mainly the synthesis based on molten salt requires high temperatures which is a solid state reactions. The heating conditions such as temperature and duration are determined by the desired powder characteristics. In general the rate of material transport is increased with an increase in the heating temperature. At the same time, the salt evaporation increases as well. The heating duration is determined by the reaction rate and the size and shape of the product particles. In a particular system, the heating rate influences the size of the product particles such as shape and chemical composition of the precursors involved are all important, synthesis need to be carried out at a temperature where the flux is a liquid. Purity problems can arise, due to incorporation of the molten salt ions in the product. This can be overcome either by using a salt containing cations and/or anions which are also present in the desired product.

Another key factor need to concern is product morphology. Whereas sample prepared at 800°C gave more agglomeration of the particles. So while choosing the annealing temperature melting point of the sample need to take into consideration. Sample prepared at 600°C possessed varying high agglomeration of spherical particles. In fact, the percentage of spheres increased

temperature from 600°C to 700°C. Hence, these initial observations, which are consistent with our previous data, suggest that higher annealing temperatures and reaction times are conducive to the production of relatively pure, spherically shaped $\text{La}_2\text{NiMnO}_6$ samples.

Molten salt synthesis (MSS) as a large scale, one-step, rapid and environmentally friendly method for preparing functional materials, has been considerable interest. The main processing steps involved in MSS method are described in Table 2. Essentially lanthanum nickel manganese precursors corresponding to the desired compound are mixed with either the desired salts such as NaCl/KCl and then heated at a temperature above the melting point of the salt medium to form a molten flux. At this temperature, precursor materials disperse, dissociate, rearrange and then diffuse rapidly throughout the salt. Upon further heating, particles of the desired metal-oxide phase are formed through an initial nucleation step followed by a growth process that is very much dependant upon the identity of the salt species, the quantity of salt used in the reaction medium, the magnitude of the temperature at which the reaction is run, and the reaction duration. After cooling, the salt itself can be typically and rather eliminated by washing with deionized water. Upon drying, unagglomerated powders can be routinely obtained after appropriate processing (Philip 2001).

Table 2. Flow chart illustrating factors influencing the molten-salt synthesis of transition metal oxide materials (Mao et al. 2007).

Processing step	Factors effect on the nanoparticle
Precursor materials	Initial particle size, shape, geometry, morphology and purity of precursors
Mixing of precursor molecules with salts	Chemical nature and quality of salts, purity of slats
Annealing temperature	Synthesis temperature/reaction time, heating and cooling rates
Washing of salt mixture with sample	Remaining impurities from salt and precursor components
Drying	Presence of agglomerates

CHAPTER IV

CONCLUSION

$\text{La}_2\text{NiMnO}_6$ was successfully prepared by facile sol-gel molten-salt synthesis process which is a new approach for making orthorhombic structure of these polycrystalline samples without obvious centering at the submicron size scale. In this method we are using sol-gel method for making precursor in the form of a gel and mixing with the nitrate salts followed by synthesized via molten salt synthesis procedure because the MSS method is one of the simplest, more versatile and highly cost-effective approaches available for obtaining crystalline, chemically pure, single-phase nanoscale materials at relative lower temperatures and often in overall shorter reaction times with little residual impurities as compared with conventional solid-state reactions. These samples were prepared at 700°C . NaNO_3 and KNO_3 salts act as wetting agents in MSS method which render more effective to reduce the surface tension between the precursors during phase transformation of solid into liquid while heating and spreading over and penetrating surfaces. Here the nitrate salts and the eutectic mixture are heated above the melting point of the salt. The intrinsic scalability, flexibility and facility of this technique render it attractive for the fabrication of a range of materials. Here the synthesis method followed was a kind of modifying sol-gel molten salt synthesis which was a new kind of approach. Characterization by means of XRD, SEM, Raman spectroscopy data confirmed the formation of

$\text{La}_2\text{NiMnO}_6$ nanoparticles. The electrochemical performances was carried in order to study the oxygen evolution properties which shows its better stability and activity measurements at high overpotential required to store the energy. In order to have better OER properties it is important to understand the intrinsic properties of the perovskite oxides.

CHAPTER V

FUTURE ENDEAVORS

A major scientific challenge facing the world today remains in developing double perovskites for renewable energy sources, of which finding the potential electrocatalyst for oxygen evolution reactions is one promising pathway to exploit sunlight and water, two abundant sources, and store energy in the form of chemical bonds. The discovery of highly active and cost-effective catalysts for the oxygen evolution reaction (OER) is a key challenge for any energy storage devices. Firstly, extensive work should be done on Lanthanum based nanoparticle systems. It would be interesting to see how these transition metal oxides would react if we change the A and B site transition metal atoms with other atoms such as cobalt and manganese instead of nickel and manganese. And more research should be done on the lanthanum nickel manganese oxide material in ways of synthesizing by using various approaches and how these synthesized particles are going to effect the photocatalysis properties. However, wide scale use of any compound has been limited due to efficiency and affordability. How do we can overcome these important points? In order to have better electrochemical performance the material should withstand its stability and activity. These are the main concerns in developing alternative electrocatalysts for future research activities. So, in regard of this aspect the lanthanum based materials should undergo further characterization, preferably by thermal analysis of TGA and

DSC. In this study as TEM analysis has to be carried in order to have better information on characteristics of particle size. Our work focus on mainly synthesizing the nanoparticle by molten salt synthesis need further and tested for electrochemical performance. Continued fundamental research will be necessary in order to gain understanding at the basic level such as oxide surface chemistry and how these particles are changing its crystalline structure under repetitive cyclings. This could be carried by characterizing the cycling samples for Raman spectroscopy studies and X-Ray photoelectron spectroscopy studies.

The synthesis process outlined in this thesis is versatile and can be used for synthesizing other double and triple perovskite nanostructures is a promising energy storage device. Also one of our main focus is to synthesize $\text{La}_2\text{NiMnO}_6$ nanoparticle by molten salt synthesis and characterized by using SEM and Raman studies. Its electrochemical performance was carried out by performing cyclic voltammetry to study its stability and activity studies.

REFERENCES

- Betley TA, Wu Q, Van Voorhis T, Nocera DG (2008) Electronic design criteria for O–O bond formation via metal–oxo complexes. *Inorganic chemistry* 47 (6):1849-1861
- Bockris JOM, Otagawa T (1984) The electrocatalysis of oxygen evolution on perovskites. *Journal of the Electrochemical Society* 131 (2):290-302
- Brinker CJ, Scherer GW (2013) *Sol-gel science: the physics and chemistry of sol-gel processing*. Academic press
- Chen C-F, King G, Dickerson RM, Papin PA, Gupta S, Kellogg WR, Wu G (2015) Oxygen-deficient BaTiO_3^{-x} perovskite as an efficient bifunctional oxygen electrocatalyst. *Nano Energy* 13 (0):423-432
- Crepaldi EL, Pavan PC, Valim JB (2000) Comparative study of the coprecipitation methods for the preparation of layered double hydroxides. *Journal of the Brazilian Chemical Society* 11 (1):64-70
- Demazeau G Solvothermal processes: new trends in materials chemistry. In: *Journal of Physics: Conference Series*, 2008. vol 8. IOP Publishing, p 082003
- Garcia E, Li Q, Sun X, Lozano K, Mao Y (2015) TiO_2 Fibers: Tunable Polymorphic Phase Transformation and Electrochemical Properties. *Journal of Nanoscience and Nanotechnology* 15 (5):3750-3756
- Ge B, Ma JT, Ai DS, Lin XP, Deng CS Preparation of Double-Perovskites $\text{Sr}_2\text{Fe}_{1-x}\text{Sc}_x\text{MoO}_{6-\delta}$ Powders for the Cathode of SOEC by Sol-Gel Citrate Method. In: *Advanced Materials Research*, 2010. Trans Tech Publ, pp 657-659
- Grimaud A, Carlton CE, Risch M, Hong WT, May KJ, Shao-Horn Y (2013a) Oxygen Evolution Activity and Stability of $\text{Ba}_6\text{Mn}_5\text{O}_{16}$, $\text{Sr}_4\text{Mn}_2\text{CoO}_9$, and $\text{Sr}_6\text{Co}_5\text{O}_{15}$: The Influence of Transition Metal Coordination. *The Journal of Physical Chemistry C* 117 (49):25926-25932
- Grimaud A, May KJ, Carlton CE, Lee Y-L, Risch M, Hong WT, Zhou J, Shao-Horn Y (2013b) Double perovskites as a family of highly active catalysts for oxygen evolution in alkaline solution. *Nat Commun* 4

- Guo H, Burgess J, Street S, Gupta A, Calvarese T, Subramanian M (2006) Growth of epitaxial thin films of the ordered double perovskite $\text{La}_2\text{NiMnO}_6$ on different substrates. *Applied Physics Letters* 89 (2):022509
- Hardin WG, Slanac DA, Wang X, Dai S, Johnston KP, Stevenson KJ (2013) Highly Active, Nonprecious Metal Perovskite Electrocatalysts for Bifunctional Metal–Air Battery Electrodes. *The Journal of Physical Chemistry Letters* 4 (8):1254-1259
- Hench LL, West JK (1990) The sol-gel process. *Chemical Reviews* 90 (1):33-72
- Hong WT, Risch M, Stoerzinger KA, Grimaud A, Suntivich J, Shao-Horn Y (2015) Toward the rational design of non-precious transition metal oxides for oxygen electrocatalysis. *Energy & Environmental Science* 8:1404-1427
- Iliev M, Abrashev M, Popov V, Hadjiev V (2003) Role of Jahn-Teller disorder in Raman scattering of mixed-valence manganites. *Physical Review B* 67 (21):212301
- Jeong U, Teng X, Wang Y, Yang H, Xia Y (2007) Superparamagnetic colloids: controlled synthesis and niche applications. *Advanced Material* 19 (1):33
- Jin M, Zhang X, Qiu Ye, Sheng J (2010) Layered $\text{PrBaCo}_2\text{O}_{5+\delta}$ perovskite as a cathode for proton-conducting solid oxide fuel cells. *Journal of Alloys and Compounds* 494 (1–2):359-361
- Kanan MW, Nocera DG (2008) In situ formation of an oxygen-evolving catalyst in neutral water containing phosphate and Co^{2+} . *Science* 321 (5892):1072-1075
- Kim J, Yin X, Tsao K-C, Fang S, Yang H (2014) $\text{Ca}_2\text{Mn}_2\text{O}_5$ as Oxygen-Deficient Perovskite Electrocatalyst for Oxygen Evolution Reaction. *Journal of the American Chemical Society* 136 (42):14646-14649
- Lewis NS, Nocera DG (2006) Powering the planet: Chemical challenges in solar energy utilization. *Proceedings of the National Academy of Sciences* 103 (43):15729-15735
- Maiti RP, Dutta S, Mukherjee M, Mitra MK, Chakravorty D (2012) Magnetic and dielectric properties of sol-gel derived nanoparticles of double perovskite Y_2NiMnO_6 . *Journal of Applied Physics* 112 (4):044311
- Mao Y (2012) Facile molten-salt synthesis of double perovskite La_2BMnO_6 nanoparticles. *RSC Advances* 2 (33):12675-12678
- Mao Y, Park T-J, Zhang F, Zhou H, Wong SS (2007) Environmentally Friendly Methodologies of Nanostructure Synthesis. *Small* 3 (7):1122-1139
- Markovich V, Fita I, Wisniewski A, Puzniak R, Mogilyansky D, Iwanowski P, Dluzewski P, Gorodetsky G (2011) Nanometer size effect on magnetic properties of $\text{Sm}_{0.8}\text{Ca}_{0.2}\text{MnO}_3$ nanoparticles. *The Journal of Physical Chemistry C* 116 (1):435-447

- Martín-Carrón L, De Andres A, Martínez-Lope M, Casais M, Alonso J (2002) Raman phonons as a probe of disorder, fluctuations, and local structure in doped and undoped orthorhombic and rhombohedral manganites. *Physical Review B* 66 (17):174303
- Mavros MG, Tsuchimochi T, Kowalczyk T, McIsaac A, Wang L-P, Voorhis TV (2014) What Can Density Functional Theory Tell Us about Artificial Catalytic Water Splitting? *Inorganic chemistry* 53 (13):6386-6397
- McBain SC, Yiu HHP, Dobson J (2008) Magnetic nanoparticles for gene and drug delivery. *International Journal of Nanomedicine* 3 (2):169-180
- Mueller DN, Machala ML, Bluhm H, Chueh WC (2015) Redox activity of surface oxygen anions in oxygen-deficient perovskite oxides during electrochemical reactions. *Nat Commun* 6
- Neburchilov V, Wang H, Martin JJ, Qu W (2010) A review on air cathodes for zinc–air fuel cells. *Journal of Power Sources* 195 (5):1271-1291
- Nishio K, Ikeda M, Gokon N, Tsubouchi S, Narimatsu H, Mochizuki Y, Sakamoto S, Sandhu A, Abe M, Handa H (2007) Preparation of size-controlled (30–100nm) magnetite nanoparticles for biomedical applications. *Journal of Magnetism and Magnetic Materials* 310 (2):2408-2410
- Philip M (2001) Nanostructured materials. *Reports on Progress in Physics* 64 (3):297
- Pickett WE, Moodera JS (2001) Half metallic magnets. *Physics Today* 54 (5):39-45
- Rincón RA, Ventosa E, Tietz F, Masa J, Seisel S, Kuznetsov V, Schuhmann W (2014) Evaluation of Perovskites as Electrocatalysts for the Oxygen Evolution Reaction. *ChemPhysChem* 15 (13):2810-2816
- Rogado NS, Li J, Sleight AW, Subramanian MA (2005) Magnetocapacitance and Magnetoresistance Near Room Temperature in a Ferromagnetic Semiconductor: $\text{La}_2\text{NiMnO}_6$. *Advanced Materials* 17 (18):2225-2227
- Singh MP, Charpentier S, Truong KD, Fournier P (2007a) Evidence of bidomain structure in double-perovskite $\text{La}_2\text{CoMnO}_6$ thin films. *Applied Physics Letters* 90 (21):211915
- Singh MP, Grygiel C, Sheets WC, Boullay P, Hervieu M, Prellier W, Mercey B, Simon C, Raveau B (2007b) Absence of long-range Ni/Mn ordering in ferromagnetic $\text{La}_2\text{NiMnO}_6$ thin films. *Applied Physics Letters* 91 (1):012503
- Spendelow JS, Wieckowski A (2007) Electrocatalysis of oxygen reduction and small alcohol oxidation in alkaline media. *Physical Chemistry Chemical Physics* 9 (21):2654-2675

- Stoerzinger KA, Choi WS, Jeon H, Lee HN, Shao-Horn Y (2015) Role of Strain and Conductivity in Oxygen Electrocatalysis on LaCoO₃ Thin Films. *The Journal of Physical Chemistry Letters* 6 (3):487-492
- Suntivich J, Gasteiger HA, Yabuuchi N, Nakanishi H, Goodenough JB, Shao-Horn Y (2011a) Design principles for oxygen-reduction activity on perovskite oxide catalysts for fuel cells and metal–air batteries. *Nat Chem* 3 (7):546-550
- Suntivich J, May KJ, Gasteiger HA, Goodenough JB, Shao-Horn Y (2011b) A Perovskite Oxide Optimized for Oxygen Evolution Catalysis from Molecular Orbital Principles. *Science* 334 (6061):1383-1385
- Tang D, Yuan R, Chai Y (2006) Magnetic Core–Shell Fe₃O₄@Ag Nanoparticles Coated Carbon Paste Interface for Studies of Carcinoembryonic Antigen in Clinical Immunoassay. *The Journal of Physical Chemistry B* 110 (24):11640-11646
- Thompson CM, Chi L, Hayes JR, Hallas AM, Wilson MN, Munsie TJS, Swainson IP, Grosvenor AP, Luke GM, Greedan JE (2015) Synthesis, structure, and magnetic properties of novel B-site ordered double perovskites, SrLaMReO₆ (M = Mg, Mn, Co and Ni). *Dalton Transactions* 44 (23):10806-10816
- Trasatti S (1980) Electrocatalysis by oxides—attempt at a unifying approach. *Journal of Electroanalytical Chemistry and Interfacial Electrochemistry* 111 (1):125-131
- Trasatti S (1984) Electrocatalysis in the anodic evolution of oxygen and chlorine. *Electrochimica Acta* 29 (11):1503-1512
- Tseung A, Jasem S (1977) Oxygen evolution on semiconducting oxides. *Electrochimica Acta* 22 (1):31-34
- Tsipis EV, Kharton VV (2011) Electrode materials and reaction mechanisms in solid oxide fuel cells: a brief review. III. Recent trends and selected methodological aspects. *Journal of Solid State Electrochemistry* 15 (5):1007-1040
- Wold A, Arnott R, Goodenough J (1958) Some Magnetic and Crystallographic Properties of the System LaMn_{1-x}Ni_xO_{3+λ}. *Journal of Applied Physics* 29 (3):387-389
- Yokoyama Y, Ootsuki D, Sugimoto T, Wadati H, Okabayashi J, Yang X, Du F, Chen G, Mizokawa T (2015) Electronic structure of Li_{1+x}[Mn_{0.5}Ni_{0.5}]_{1-x}O₂ studied by photoemission and x-ray absorption spectroscopy. *Applied Physics Letters* 107 (3):033903
- Zhang C, Zhang T, Ge L, Wang S, Yuan H, Feng S (2014) Hydrothermal synthesis and multiferroic properties of Y₂NiMnO₆. *RSC Advances* 4 (92):50969-50974

Zhang Z, Jian H, Tang X, Yang J, Zhu X, Sun Y (2012) Synthesis and characterization of ordered and disordered polycrystalline $\text{La}_2\text{NiMnO}_6$ thin films by sol-gel. Dalton Transactions 41 (38):11836-11840

Zhou J, Zhang S, Qiao X, Li X, Wu L (2006) Synthesis of SiO_2 /poly (styrene-co-butyl acrylate) nanocomposite microspheres via miniemulsion polymerization. Journal of Polymer Science Part A: Polymer Chemistry 44 (10):3202-3209

BIOGRAPHICAL SKETCH

Padmini Kukkapalli, was born on March 03, 1992, in Andhra Pradesh, India. She was single daughter to her parents Srinivasa Rao Kukkapalli, and Vanajakshi Kukkapalli. She obtained her high school degree from Vignan Steel city Public school Visakhapatnam in 2007. She obtained her college degree from Narayana Junior college Vijayawada in 2009. Later she graduated from Jawaharlal Technological University-kakinada in 2013 with Bachelor's degree in Pharmacy. She works at NATCO pharmacy for 6months and moved to US in 2014 and she was accepted to the University of Texas Rio Grande Valley to obtain in 2014 in order to pursue Masters degree in Chemistry. There she started working as a graduate assistant while working on reserach with Dr.Yuanbing Mao on her thesis topic, Facile sol-gel molten-salt synthesis of double perovskite $\text{La}_2\text{NiMnO}_6$ as anelectrocatalyst for oxygen evolution reactions. Sherecieved a Masters degree in December 2015.

Her Permanent Address is:

Padmini Kukkapalli

F/O Srinivasa Rao Kukkapalli

Yenamalakuduru

Vijayawada

Andhra Pradesh

India.